

Magnetohydrodynamic Simulation of Kink Instability and Plasma Flow during Sustainment of a Coaxial Gun Spheromak

Takashi KANKI, Masayoshi NAGATA¹⁾ and Yasuhiro KAGEI²⁾

Department of Maritime Science and Technology, Japan Coast Guard Academy, Kure, Hiroshima 737-8512, Japan

¹⁾*Department of Electrical Engineering and Computer Sciences, University of Hyogo, Himeji, Hyogo 671-2280, Japan*

²⁾*Research Organization for Information Science & Technology, Tokai, Ibaraki 319-1106, Japan*

(Received 5 December 2009 / Accepted 15 March 2010)

Kink instability and the subsequent plasma flow during the sustainment of a coaxial gun spheromak are investigated by three-dimensional nonlinear magnetohydrodynamic simulations. Analysis of the parallel current density λ profile in the central open column revealed that the $n = 1$ mode structure plays an important role in the relaxation and current drive. The toroidal flow ($v_t \approx 37$ km/s) is driven by magnetic reconnection occurring as a result of the helical kink distortion of the central open column during repetitive plasmoid ejection and merging.

© 2010 The Japan Society of Plasma Science and Nuclear Fusion Research

Keywords: spheromak, coaxial helicity injection, MHD relaxation, kink instability, plasma flow, simulation

DOI: 10.1585/pfr.5.S2055

1. Introduction

Taylor's magnetohydrodynamic (MHD) relaxation theory [1] states that a turbulent MHD system relaxes to a minimum magnetic energy state subject to the constraint that the global magnetic helicity is conserved, but it provides no mechanism for how the relaxation occurs and how the toroidal plasma current is driven. Toroidal plasmas with a low safety factor q profile such as spheromaks [2] and reversed-field pinches (RFPs) [3], which tend to easily self-organize, are traditionally the object of study for relaxation physics. Many spheromak experiments have been performed with the objective of understanding the relaxation and current drive mechanism using a magnetized coaxial plasma gun (MCPG), i.e., a helicity injector [4, 5]. Relaxation phenomena such as plasmoid ejection, helical kinks, magnetic reconnection, and rotation are observed in helicity injection experiments as well as in solar flares and astrophysical jets. Comprehensive understanding of the relaxation mechanism underlying the physics in the helicity injection system is of fundamental importance for both laboratory and space plasmas.

Recently, the repetitive plasmoid ejection and merging model, in which the plasma flow ejected from the MCPG may play an important role, is proposed as a possible current drive mechanism [6]. The validity of this model has been verified in the Helicity Injected Spherical Torus (HIST) device [7] using a fast-framing camera, internal magnetic probe, and Mach probe. The fast camera reveals helical kink distortion in the open flux around the central conductor. The intermittent plasma ion flow (20-40 km/s) observed by the Mach probe is correlated with fluctuations in the electron density, toroidal current, and toroidal

mode number $n = 1$ mode. Experiments must be compared to numerical simulations. We investigate the fundamental physics of the MHD relaxation process and current drive using three-dimensional (3D) nonlinear MHD simulations [8, 9]. In this paper, we focus on the helical kink instability and subsequent plasma flow driven by magnetic reconnection during sustainment of a coaxial gun spheromak.

2. Simulation Model

The helical distortion noted in Section 1 usually appears to be a nonaxisymmetric. Therefore, a 3D simulation geometry is essential to reproduce the distortion properly. All variables are treated in a normalized form. The length, magnetic field, and number density are normalized by the maximum length of the cylinder radius, $L_0 = 0.5$ m, the strength of the characteristic magnetic field, $B_0 = 0.2$ T, and the initial ion number density in the hydrogen plasma, $n_0 = 5.0 \times 10^{19} \text{ m}^{-3}$, respectively. Under these normalizations, the velocity and time are normalized by the Alfvén velocity, $v_A = 620$ km/s, and the Alfvén transit time, $\tau_A = 0.81 \mu\text{sec}$, respectively. We adopt the simulation system shown in Fig. 1 and use a 3D full-toroidal cylindrical (r, θ, z) geometry. We divide the simulation region into two cylinders with a central conductor inserted along the symmetry axis. One is a gun region ($0.175 \leq r \leq 0.65$ and $0 \leq z \leq 0.5$) corresponding to the MCPG region. The other is a confinement region ($0.15 \leq r \leq 1.0$ and $0.5 \leq z \leq 2.0$). The insertion of a toroidal field current I_{tf} along the geometry axis inside the central conductor produces a vacuum toroidal field, creating a tokamak configuration. In this paper, we set $I_{\text{tf}} = 0$ because we consider a spheromak configuration.

author's e-mail: kanki@jcga.ac.jp

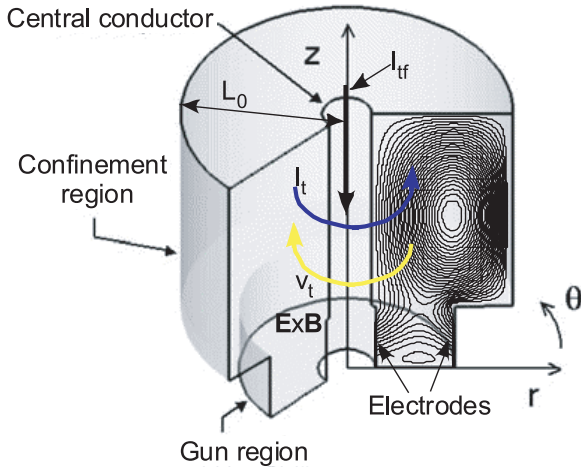


Fig. 1 Schematic view of simulation geometry in cylindrical coordinates (r, θ, z) . Blue arrow indicates the direction of toroidal current I_t , and yellow arrow indicates that of toroidal velocity v_t and $\mathbf{E} \times \mathbf{B}$ plasma rotation.

The governing equations to be solved in the simulation are the set of nonlinear resistive MHD equations:

$$\frac{\partial \rho \mathbf{v}}{\partial t} = -\nabla \cdot \rho \mathbf{v} \mathbf{v} + \mathbf{j} \times \mathbf{B} - \nabla p - \nabla \cdot \vec{\mathbf{H}}, \quad (1)$$

$$\frac{\partial \mathbf{B}}{\partial t} = -\nabla \times \mathbf{E}, \quad (2)$$

$$\frac{\partial p}{\partial t} = -\nabla \cdot (\rho \mathbf{v} - \kappa \nabla T) - (\gamma - 1)(\rho \nabla \cdot \mathbf{v} + \vec{\mathbf{H}} : \nabla \mathbf{v} - \eta j^2), \quad (3)$$

$$\mathbf{E} = -\mathbf{v} \times \mathbf{B} + \eta \mathbf{j}, \quad (4)$$

$$\mathbf{j} = \nabla \times \mathbf{B}, \quad (5)$$

$$T = \frac{p}{\rho}, \quad (6)$$

$$\vec{\mathbf{H}} = \mu \left(\frac{2}{3} (\nabla \cdot \mathbf{v}) \vec{\mathbf{I}} - \nabla \mathbf{v} - {}^t(\nabla \mathbf{v}) \right), \quad (7)$$

where ρ is mass density, \mathbf{v} is fluid velocity, \mathbf{B} is magnetic field, and p is plasma pressure. For simplicity, the conductivity κ , viscosity μ , and resistivity η are assumed to be uniformly constant throughout the entire region. The ratio of specific heats γ is 5/3.

To solve the equations, we use the second-order finite differences method for the spatial derivatives and the fourth-order Runge-Kutta method for time integration. The grid numbers are set to $(N_r, N_\theta, N_z) = (39, 64, 40)$ in the gun region and $(N_r, N_\theta, N_z) = (69, 64, 121)$ in the confinement region. A bias magnetic flux penetrates electrodes at the inner and outer boundaries of the gun region to drive the plasma current by applying an electric field. We use a perfect conducting boundary at the wall of the confinement region. The initial conditions for the simulation are given by an axisymmetric MHD equilibrium, which can be obtained by numerically solving a Grad-Shafranov equation derived from a force-free relation, $\nabla \times \mathbf{B} = \lambda \mathbf{B}$

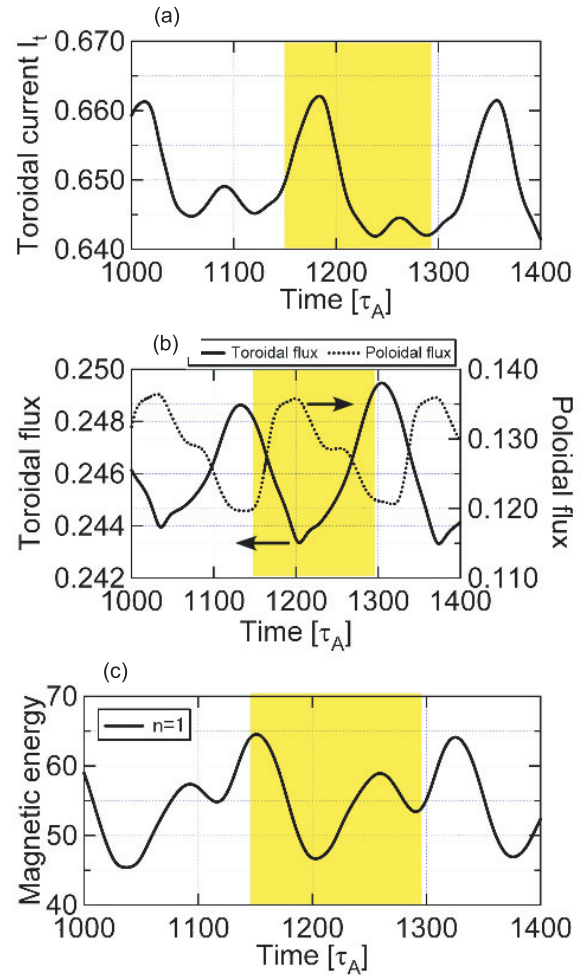


Fig. 2 Time evolutions of the toroidal current (a), magnetic flux (b), and magnetic energy for the toroidal Fourier mode $n = 1$ (c).

under these boundary conditions. Here λ is the force-free parameter, defined by $\lambda \equiv \mathbf{j} \cdot \mathbf{B} / B^2$, representing the current density parallel to the magnetic field. In the simulation, the mass density is spatially and temporally constant, and no-slip wall condition, $\mathbf{v} = 0$, is assumed at all boundaries of the simulation region.

3. Simulation Results

On the basis of the simulation results for the sustainment of a coaxial gun spheromak, the physical description of kinking behavior and plasma flow is investigated. The parameters used in the simulation are force-free parameters at the magnetic axis, $\lambda_{\text{axis}} = -4.8$, and at the separatrix, $\lambda_s = -4.7$, and the safety factors at the magnetic axis, $q_{\text{axis}} = 0.74$ and at the separatrix, $q_s = 0.59$, corresponding to a partially relaxed spheromak configuration. The poloidal flux contours with the axisymmetric MHD equilibrium used as the initial condition are shown in Fig. 1. In addition, κ , μ , and η are assumed to be 1.0×10^{-3} , 1.0×10^{-3} , and 2.0×10^{-4} , respectively. A toroidally symmetric radial electric field E_{inj} of 3.0×10^{-3} is always ap-

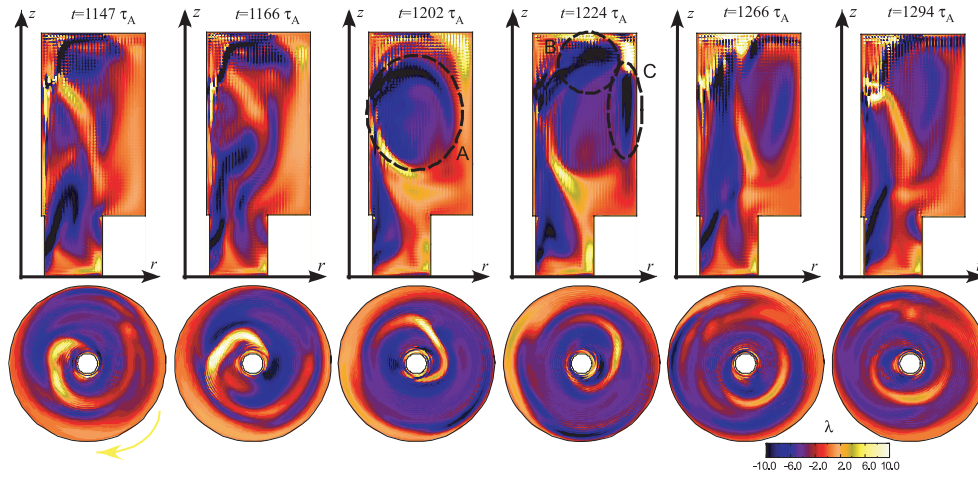


Fig. 3 Time evolution of contours of λ on the poloidal cross section at the $\theta = 3\pi/2$ plane and toroidal cross section at the midplane. Color of λ varies from black to blue, red, yellow, and white as λ increases.

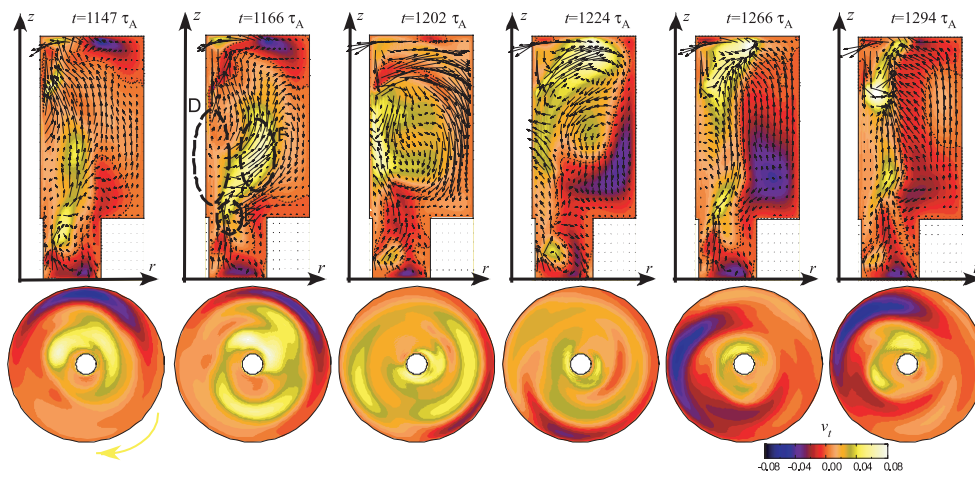


Fig. 4 Time evolution of vector plots of poloidal flow velocity v_p and contours of toroidal flow velocity v_t on the poloidal cross section at the $\theta = 3\pi/2$ plane and toroidal cross section at the midplane, respectively. Color of v_t varies from black to blue, red, yellow, and white as v_t increases.

plied to the gap between gun electrodes during the simulation.

Figure 2 shows the time evolution of the toroidal current I_t , toroidal magnetic flux Ψ_t , poloidal magnetic flux Ψ_p , and magnetic energy W_{mag} for the toroidal Fourier mode $n = 1$ during the sustainment time range. As shown in Fig. 2(a), I_t is successfully sustained against resistive decay, and I_t , Ψ_t , Ψ_p , and W_{mag} have periodic oscillations. The oscillations of I_t and Ψ_p are very well correlated. The oscillations of Ψ_p are out of phase with those of Ψ_t and W_{mag} because Ψ_p reaches a maximum at the bottom of Ψ_t and W_{mag} . This means that the flux conversion from Ψ_t to Ψ_p occurs during the sustainment and is related to the oscillations of the $n = 1$ mode. The plasma with this $n = 1$ helical magnetic distortion rotates in the toroidal direction with the frequency $f \approx 16$ kHz, calculated by the phase development of I_t on the poloidal cross sections at $\theta = 0, \pi/2, \pi$, and $3\pi/2$ planes. This plasma rotation due to $\mathbf{E} \times \mathbf{B}$

drift driven by the applied E_{inj} is in the opposite direction to I_t . This result from internal magnetic probe measurements agrees with observations in the HIST operated in the spheromak mode ($I_{\text{rf}} = 0$) [7].

The sustained spheromak dynamics with helical distortion of the open magnetic field lines around the central conductor, i.e., the central open column, has been investigated by vector plots of the poloidal magnetic field, B_p , and contours of the toroidal field, B_t , in a previous study [9]. When the poloidal gun current along the central open column is increased by a continuously applied E_{inj} , a critical current density gradient is attained, and the central open column violates the Kruskal-Shafranov kink stability criterion [10]. The $n = 1$ kink mode of the central open column is destabilized, leading to the experimentally observed helical distortion [7, 11].

Figure 3 shows the time evolution of λ on the toroidal and poloidal cross sections in the yellow time range of

Fig. 2. At $t = 1147 \tau_A$, the $n = 1$ kink instability causes a strong helical distortion of λ winding around the central conductor. Plasma is also ejected from the gun region with rotation in the toroidal direction due to the $\mathbf{E} \times \mathbf{B}$ drift. The twist direction is right handed from the confinement region side, corresponding to the direction of $\mathbf{j}_{\text{gun}} \times \mathbf{B}_{\text{bias}}$, where \mathbf{j}_{gun} and \mathbf{B}_{bias} are the gun current density and bias poloidal field, respectively. λ is always provided from the gun to the confinement region and has the same direction as I_t (blue) except for the current sheet (yellow) around the central conductor. The current sheet is generated by the twisting of magnetic field lines. At $t = 1202 \tau_A$, a detached λ region (A) is produced by a magnetic reconnection event that generates plasmoid-like closed poloidal field lines, and then this region relaxes to the axisymmetric state except for the presence of the current sheet. At $t = 1224 \tau_A$, the upper part of the helical distortion of λ (B) is strongly displaced from the geometric axis, and a return of λ near the outboard (C) appears, similar to the hook-shaped structure observed in the Spheromak Experiment (SPHEX) device [11].

Figure 4 shows vector plots of poloidal flow velocity v_p and contours of toroidal flow velocity v_t on the toroidal and poloidal cross sections, respectively. The poloidal cross section reveals that the plasma with the $n = 1$ helical distortion around the central conductor (D) moves to the confinement region at $t = 1166 \tau_A$ [9]. As a result, a magnetic reconnection event occurs at the X-point near the gun muzzle (E), and the positive toroidal flow (yellow) of $v_t \approx 37 \text{ km/s}$ (F) is driven in the opposite direction to I_t , but in the same direction as the $\mathbf{E} \times \mathbf{B}$ plasma rotation. This result is consistent with the flow observed in the Helicity Injected Torus (HIT-II) [12] and the National Spherical Torus Experiment (NSTX) [13]. At $t = 1202 \tau_A$, this magnetic reconnection event generates closed poloidal field lines, which are in a partially relaxed state with a strong poloidal flow in the periphery region. In the next stage, the positive toroidal flow driven by magnetic reconnection remains at the inboard, while intense new negative toroidal flow (blue) is induced at the outboard. This new plasma flow may be associated with the anti-dynamo effect. Then new plasma is ejected from the gun region, and this process is repeated with at a time interval of $\sim 170 \tau_A$. The toroidal cross section at $t = 1147 \tau_A$ reveals that positive toroidal flow exists around the central conductor, and

negative flow exists at the outboard side. At $t = 1166 \tau_A$, the positive flow region expands toward the outboard side, while the negative one gradually becomes small. At $t = 1202 \tau_A$, positive flow occupies almost the entire region. After $t = 1224 \tau_A$, negative flow is enhanced again, and positive flow is gradually suppressed.

4. Summary and Conclusions

By using 3D nonlinear MHD simulations, we have investigated the helical kink instability and subsequent plasma flow driven by magnetic reconnection during the sustainment of a coaxial gun spheromak. Analysis of the λ profile with helical kink distortion in the central open column reveals that a rotating $n = 1$ mode structure plays an important role in the relaxation and current drive. The toroidal flow ($v_t \approx 37 \text{ km/s}$) is driven by the magnetic reconnection occurring at the X-point due to the helical kink distortion of the central open column during repetitive plasmoid ejection and merging. This flow direction is opposite to I_t , but the same as the $\mathbf{E} \times \mathbf{B}$ drift. This result is consistent with the flow observed in coaxial helicity injection experiments. Interestingly, positive and negative toroidal flows coexist in the toroidal cross section. When I_t is relatively large, the positive flow is enhanced, suggesting a dynamo current drive.

- [1] J.B. Taylor, *Rev. Mod. Phys.* **58**, 741 (1986).
- [2] T.R. Jarboe, *Phys. Plasmas* **12**, 058103 (2005).
- [3] H.A.B. Bodin and A.A. Newton, *Nucl. Fusion* **20**, 1225 (1980).
- [4] S.O. Knox *et al.*, *Phys. Rev. Lett.* **56**, 842 (1986).
- [5] M. Nagata *et al.*, *Phys. Rev. Lett.* **71**, 4342 (1993).
- [6] M. Nagata *et al.*, *Proceedings of 22nd IAEA Fusion Energy Conference* (October 13-18, 2008, Geneva) EX/P6-7.
- [7] M. Nagata *et al.*, *Phys. Plasmas* **10**, 2932 (2003).
- [8] Y. Kagei *et al.*, *J. Plasma Fusion Res.* **79**, 217 (2003).
- [9] T. Kanki *et al.*, *J. Plasma Fusion Res. SERIES* **8**, 1167 (2009).
- [10] P.M. Bellan, *Fundamentals of Plasma Physics* (Cambridge University Press, Cambridge, 2006) p.382.
- [11] R. Duck *et al.*, *Plasma Phys. Control. Fusion* **39**, 715 (1997).
- [12] K.J. McCollam and T.R. Jarboe, *Plasma Phys. Control. Fusion* **44**, 493 (2002).
- [13] M. Nagata *et al.*, *Plasma and Fusion Res.* **2**, 035 (2007).